ENVIRONMENTAL RESEARCH
LETTERS

LETTER • **OPEN ACCESS**

Global chlorophyll responses to marine heatwaves in satellite ocean color

To cite this article: Kyung Min Noh *et al* 2022 *Environ. Res. Lett.* **17** 064034

ENVIRONMENTAL RESEARCH
LETTERS

CrossMark

OPEN ACCESS

RECEIVED
12 May 2021

REVISED
12 May 2022

ACCEPTED FOR PUBLICATION
18 May 2022

PUBLISHED
7 June 2022

LETTER

Global chlorophyll responses to marine heatwaves in satellite ocean color

Kyung Min Noh[1], Hyung-Gyu Lim[1,2,*] and Jong-Seong Kug[1,*]

[1] Division of Environmental Science and Engineering, Pohang University of Science and Technology (POSTECH), Pohang, Republic of Korea
[2] Princeton University/Atmospheric and Oceanic Sciences Program, Princeton, NJ 08540, United States of America
[*] Authors to whom any correspondence should be addressed.

E-mail: hyunggyu@princeton.edu and jskug@postech.ac.kr

Keywords: phytoplankton, extreme, remote sensing, daily, seasonality

Supplementary material for this article is available online

Abstract
Marine heatwaves (MHWs), prolonged ocean temperature extremes, have been enhanced by global warming in recent decades. More intense and longer MHWs have increasingly negative impacts on marine organisms that threaten their resilience of marine ecosystems. In this study, we investigated global marine phytoplankton biomass (chlorophyll) estimated by satellite ocean color and its response to MHWs on global and regional scales. We find that MHWs typically decreases chlorophyll concentrations in the tropics and mid-latitudes, with increases at high latitudes. The magnitude of chlorophyll responses to MHWs is increased in response to higher intensity and longer duration of MHWs. We find a change in the response from negative to positive chlorophyll responses to MHWs across the 40°–50° latitude bands in both hemispheres where the strongest meridional gradient in nitrate concentration exists. In these response-changing regions, the latitudinal contrast of the chlorophyll response is more distinctive in the warm season rather than in the cold season because of the shallower climatological mixed layer. The present study highlights the global phytoplankton responses to MHWs and their sensitivity to MHWs properties that imply the importance of upper-ocean interactions between phytoplankton and the mixed-layer.

1. Introduction

The increase in anthropogenic greenhouse gas emissions warms the global ocean sea surface temperature (SST), which increases the chances of extremely warm water events (Oliver *et al* 2018). These extreme events were referred to marine heatwaves (MHWs) (Pearce *et al* 2011) and were recently defined as prolonged, discrete anomalous warm-water events (Hobday *et al* 2016). MHWs are characterized in terms of their intensity, duration, frequency, and MHW categories (Hobday *et al* 2016, 2018). Intensity, duration, and frequency of MHWs have increased globally over the last decades (Oliver *et al* 2018). Regional MHW events have been reported: 2014/15, Northeast Pacific (the 'Blob') (Bond *et al* 2015, di Lorenzo and Mantua 2016); 2019/20, the second Blob (Amaya *et al* 2020); 2015/16, Tasman Sea (Oliver *et al* 2017); 2013/14, South Atlantic Ocean (Rodrigues *et al* 2019); and the Yellow Sea (Li *et al* 2019, Lee *et al* 2020). These MHWs were generated by combinations of regional processes (e.g. ocean advection, turbulent mixing, air–sea heatflux) (Vogt *et al* 2022), large-scale climate modes (e.g. El Niño–Southern Oscillation, Pacific Decadal Oscillation, Indian Ocean Dipole, etc), and teleconnections (e.g. Rossby waves, Kelvin waves, atmospheric blocking), which consist of various temporal and spatial scales in climate variabilities (Holbrook *et al* 2019). Future projections simulated in climate models suggest that more frequent and intensive MHWs are likely to occur, covering wider areas for longer periods (Frölicher *et al* 2018, Oliver *et al* 2019), suggesting that severe damage to marine ecosystems will become more prevalent.

Recently, deleterious impacts of MHWs have been reported in devastating marine ecosystems, for example, coral bleaching (Hughes *et al* 2017), toxic algal blooms (McCabe *et al* 2016, Roberts *et al* 2019), high mortality rates for seagrasses (Garrabou *et al* 2009, Arias-Ortiz *et al* 2017), seabirds (Jones *et al* 2018) and fish (Roberts *et al* 2019, Cheung and Frölicher 2020), which are all regarded as threats to biodiversity (Wernberg *et al* 2012, Smale *et al* 2019). A larger area of the ocean might be expected to be in places vulnerable to the marine ecosystem because of the widespread permanent MHW states (Oliver *et al* 2019). In particular, large marine ecosystems, where 95% of the global fisheries have been caught, may suffer from the higher intensity and annual days of MHWs in response to future warming scenarios.

Previous studies have investigated the regional impacts of MHWs in the form of case studies based on *in-situ* observations. Recently, the influence of MHWs on phytoplankton was investigated, focusing on specific coastal regions (Hayashida *et al* 2020) and extreme MHWs case studies (Gupta Sen *et al* 2020), suggesting that the abundance of background nitrate concentrations has affected global phytoplankton responses to unprecedented MHW events. Additionally, low chlorophyll extremes in the global ocean and high chlorophyll extremes in global lakes have been reported in response to high temperature events (le Grix *et al* 2021, Woolway *et al* 2021). Recently, the compound events of the other biogeochemical extremes such as deoxygenation and acidification with MHWs have become common in the future, which may intensify the detrimental impacts on marine organisms and ecosystems (Gruber *et al* 2021).

To identify the general responses of phytoplankton to MHWs and quantify the impacts of MHW properties on phytoplankton, we investigated the relationship between extreme SST and anomalous chlorophyll, a proxy for phytoplankton biomass obtained from a satellite-derived global ocean color dataset for 22 years (1998–2019). Detailed descriptions of the observational dataset are provided in section 2. The methods for defining MHWs and composite analysis with different spatial and temporal scales are described in section 3. The results of chlorophyll responses to MHWs are presented in section 4. Finally, a summary and discussion of the implications and future directions of MHW impacts on phytoplankton are provided in section 5.

2. Data

We used the National Oceanic and Atmospheric Administration (NOAA) 1/4° Optimum Interpolation daily SST version 2 (Reynolds *et al* 2007, Banzon *et al* 2016) for the period 1982–2019 (NOAA Physical Sciences Laboratory, www.esrl.noaa.gov/psd). High-resolution chlorophyll satellite observations were obtained using eight-day averaged daily Ocean Colour Climate Change Initiative data for 1998–2019 (https://esa-oceancolour-cci.org), generated by the European Space Agency (ESA) Climate Change Initiative project, which incorporated a combination of the ESA's MERIS and the National Aeronautics and Space Administration's SeaWiFS, MODIS, and VIIRS satellite data (Valente *et al* 2016). Although chlorophyll concentration is not an exact proxy for phytoplankton biomass due to the chlorophyll-to-carbon biomass ratio, it has been used as a proxy for plankton biomass (Behrenfeld *et al* 2005, Blondeau-Patissier *et al* 2014). In this study, we used chlorophyll-a concentration derived from high-resolution satellite observations to represent the variability in phytoplankton biomass. To compare the chlorophyll observations with SST data, chlorophyll data were spatially regridded to a 1/4° × 1/4° latitude/longitude grid for 1998–2019. The background nitrate concentration was obtained from the climatology of nitrate concentrations in the World Ocean Atlas 18 (Garcia *et al* 2018). The surface nitrate concentration was provided at a 1° × 1° latitude/longitude Gaussian grid, which covered the period from 1955 to 2012 based on limited *in-situ* profile data.

3. Method

SST and chlorophyll anomalies are calculated by removing the mean daily mean seasonal cycles. MHWs are defined from daily SST time series as discrete and prolonged anomalous warm-water events following a framework of Hobday *et al* (2016). In addition, MHW properties are investigated including duration, maximum intensity, frequency, and MHW exposure days, from the defined MHWs. In this study, 'discrete' means that the start and end days could be identified quantitatively, whereas 'prolonged' means that an MHW event persisted for more than five days, and 'anomalously warm water' was defined from a seasonally varying baseline climatology. A 'heatwave' event was defined as when the daily ocean temperature was higher than the 90th percentile (as a threshold) and persisted for at least five consecutive days. To separate the consecutive MHWs and ensure that the SST dropped sufficiently, the end of the MHW was determined when the daily temperature was below the 75th percentile. When the daily SST dropped below the 90th percentile and then continuously decreased until the 75th percentile, the end date of the MHW was defined as the first day below the 75th percentile. If the daily SST recovered above the 90th percentile without dropping to the 75th percentile, this was regarded as a continuation of the previous MHW (figure S1 (available online at stacks.iop.org/ERL/17/064034/mmedia)). The climatology and threshold were calculated using daily SST within an 11 days moving window and smoothed using a 31 days moving average for 1982–2012 (31 years).

Based on the above definition of an MHW event, discrete MHW properties were quantified as duration (the period between the start and end date of an MHW), maximum intensity (the maximum SST anomaly within the period of an MHW), and frequency (the number of MHWs occurring in one year). We then calculated the annually-averaged duration, maximum intensity, and frequency for each year. To clarify the effect of MHW intensity, we classified two MHW categories according to their intensity: moderate (Category 1) and strong (Category 2). The difference between the 90th percentile and climatology was defined as a unit, and the MHW was classified as Category 1 (moderate) when the temperature was between the 90th percentile (one unit) and two units. Likewise, Category 2 (strong) was defined as a temperature of more than two units (Hobday *et al* 2018).

After MHWs were globally identified by the framework at each grid point, composite analysis was performed by averaging the chlorophyll deseasonalized anomalies on MHW dates through a total time series over the last 22 years (1998–2019), following the length of the chlorophyll dataset. Because the date of MHW and the number of MHW exposure days are different in each grid (figure S2), the chlorophyll composite to MHW was calculated by averaging the chlorophyll anomalies in different MHW dates for each grid.

To bridge the gap between the time scales of daily SST and eight-day daily chlorophyll concentration, MHWs were selected according to the chlorophyll time interval (eight-day daily), and the MHW duration was calculated in multiples of eight days, which resulted in the discrete MHW duration rather than continuous duration. For example, the MHW persisted from 1 to 20 January, i.e. 20 days. The eight-day daily chlorophyll data existed at two time points in January (i.e. 8 and 16 January); therefore, the MHW duration was calculated as 16 days. To compare the impact of MHW intensity on chlorophyll, we constructed composites of chlorophyll anomalies for different MHW categories (Categories 1 and 2).

4. Results

We examine a composite pattern of chlorophyll anomalies during MHW conditions as shown in figure 1(a) (see method). In the tropical and subtropical regions, negative chlorophyll responses are mainly observed, indicating a significant decrease in phytoplankton biomass in response to MHWs. In particular, strong chlorophyll responses are captured in several regions where the magnitude of chlorophyll composite is greater than 0.03 mg m^{-3}, including in the Pacific Basin, the northern Indian Ocean, and the Atlantic Ocean. In contrast, positive chlorophyll responses are observed in the high-latitude oceans, particularly in the northern and southern Atlantic Oceans. Interestingly, the chlorophyll response to MHWs is observed to change sharply from negative to positive across the 40°–50° latitude band in both hemispheres, which is the similar pattern in simulated global chlorophyll changes under the greenhouse warming (Sarmiento *et al* 2004).

Since phytoplankton responds differently to increased temperatures depending on the dominant limiting factors, light availability and nutrient concentrations, for phytoplankton growth at different latitudes (Doney 2006), the MHW-related chlorophyll response is determined by the impact of MHWs on the limiting factors. On average, MHWs are associated with shoaling of the mixed layer at both high and low latitudes except for the eastern equatorial Pacific Ocean where the El-Niño related warming causes a lowering of the thermocline (figure S3), whereas the chlorophyll composite exhibits different chlorophyll responses to MHWs at a high and mid/low latitudes (figure 1(a)). Although the coastal regions are partially influenced by the coastal upwellings (figure S4), the different chlorophyll responses can be explained by latitudinal differences in oceanic environments, that is, the mixed layer and nutrient concentration.

In high-latitude oceans, the mixed layer is generally deep where nutrients are abundant, and the penetration depth of solar radiation (i.e. euphotic layer) is shallower than the mixed-layer depth (MLD) (Doney 2006). Meanwhile, in low-latitude oceans where mixed layers are shallower, nutrients tend to be depleted, and the euphotic layer is deeper than the MLD. In summary, light is the dominant limiting factor in high-latitude oceans, and nutrients are the dominant limiting factors in low- and mid-latitude oceans.

In the nutrient-deficient tropics and mid-latitudes, MHW-induced mixed layer shoaling (figure S3) can reduce nutrient entrainment from the deep ocean, which leads to less favorable conditions for the growth of phytoplankton. In contrast, in the nutrient-abundant high-latitude regions, stratification by MHWs increases the residence time in the euphotic layer for phytoplankton, which allows more exposure of light to phytoplankton and consequently facilitates photosynthesis (Doney 2006). Therefore, the MHW-induced weakening of vertical mixing (figure S3) leads to an increase in chlorophyll concentration in high-latitude oceans, where vertical mixing in the upper ocean is strong and nutrients are abundant (Gupta Sen *et al* 2020, Hayashida *et al* 2020). Furthermore, different latitude-dependent oceanic environments, MLD, and nutrient concentrations, are affected by enhanced stratification, resulting in the different latitude-dependent chlorophyll responses to MHWs.

The ratio of chlorophyll responses between strong MHWs and moderate MHWs is shown in figure 1(b). Figure 1(b) suggests that the intensity of chlorophyll responses to MHWs became stronger under stronger MHWs in both hemispheres. In particular, in six selected regions (shown in figure 1(a)) where

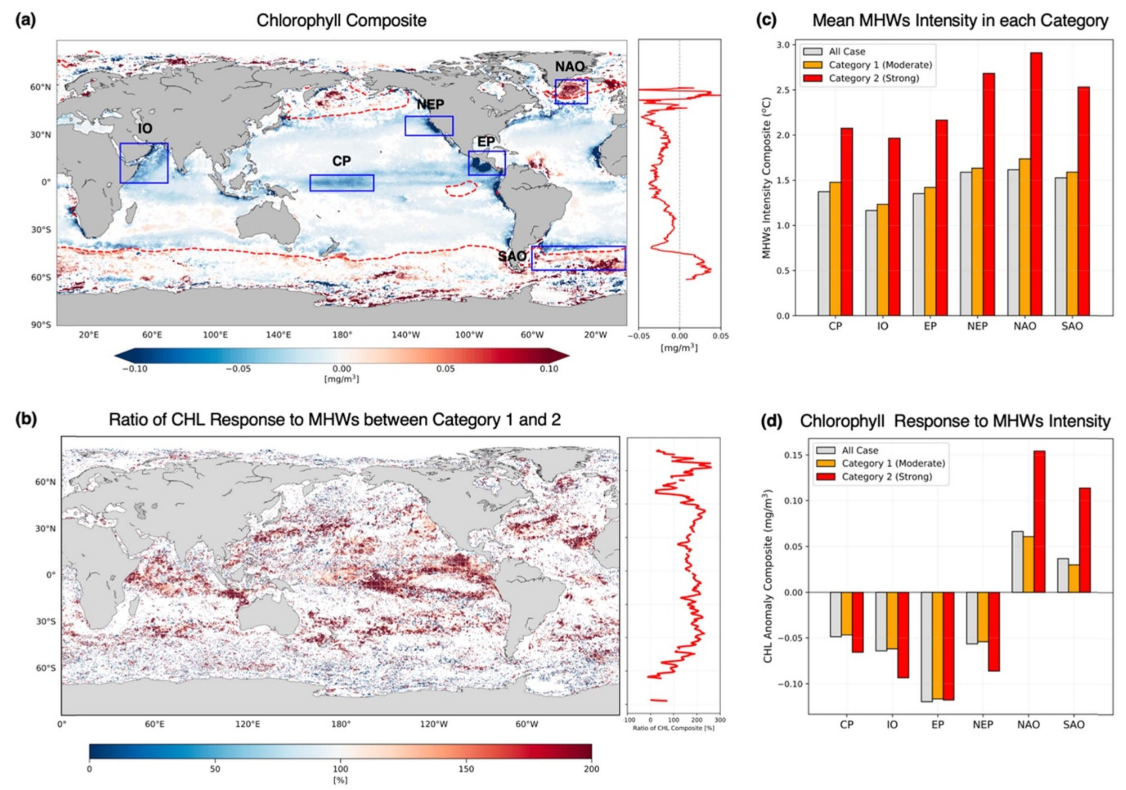

Figure 1. The impacts of MHWs on phytoplankton biomass. (a) MHW chlorophyll composites on a 1/4° grid system (1440 × 720) for the period 1998–2019, displayed only within significant regions at a 95% confidence level (calculated using a Student's *t*-test). The MHW events were calculated on each grid so that the selected date of MHWs on each grid differed. The red dashed lines represent 8 mmol m^{-3} iso-nitrate concentration lines. (b) The ratio of chlorophyll composites to strong MHWs (Category 2) and moderate MHWs (Category 1). Six regions, where chlorophyll response to MHWs is strong, are included; (c) the area-averaged MHW intensity and (d) chlorophyll composite to MHWs for each MHW category in selected significant regions—CP: Central Pacific Ocean (5° S–5° N, 160° E–160° W); IO (0°–25° N, 40°–70° E); EP: East Pacific Ocean (5°–20° N, 77°–100° W); NEP (30°–42° N, 110°–140° W); NAO: North Atlantic Ocean (50°–65° N, 25°–45° W); SAO: South Atlantic Ocean (40°–55° S, 0°–60° W).

the chlorophyll responses to MHWs are significant and strong in both anomaly value and normalized value by standard deviations (figure S5(b)), the mean MHW intensity for different MHW categories and the associated chlorophyll responses are shown in figures 1(c) and (d) for the six selected regions. All selected regions show stronger chlorophyll responses under strong MHW intensity (Category 2) than under moderate MHW intensity (Category 1), indicating that chlorophyll decreases more in the tropical and mid-latitude regions (CP, IO, EP, and NEP) and increases more in the high-latitude regions (NAO and SAO) under stronger MHW intensity.

MHW duration also affects the intensity of chlorophyll responses to MHWs. We conduct the same chlorophyll composite during MHW conditions for different MHWs durations, as shown in figures 2(a) and (b). Overall, the comparison of MHW duration impacts on chlorophyll, between the short and long durations of MHWs, represents similar spatial patterns of chlorophyll responses to MHWs: negative anomalies in the tropics and mid-latitudes regions, and positive anomalies in high-latitudes, as shown in figure 1(a). However, the significant areas in the chlorophyll composite are about two times larger in response to long duration cases compared to short duration cases. These chlorophyll responses to longer duration MHWs are more distinctive, and the patterns to have negative to positive transitions are more clear in both hemispheres.

The regional influence of increased duration of MHWs on chlorophyll responses in six selected regions is shown in figures 2(c)–(h), which represents the negative relationship between the MHW durations and the mean chlorophyll anomalies during the MHW period in the tropical and mid-latitude regions (figures 2(c), (d), (f), (g)) and the positive relationship in high-latitude oceans (figures 2(e) and (h)). The MHW impacts on chlorophyll anomalies exhibit weak responses for 20–40 days of MHWs with high variabilities. These MHW impacts are intensified to approximately 1 standard deviation of chlorophyll when the phytoplankton is exposed to MHWs for longer than 200 days. The impact of the MHWs on the mixed layer is weaker in response to the short duration cases than the long duration cases that the relationship between MHWs and chlorophyll is not robust in the short duration cases. As a result, a high-variability in chlorophyll responses exists, and the chlorophyll composite is less clear in response to

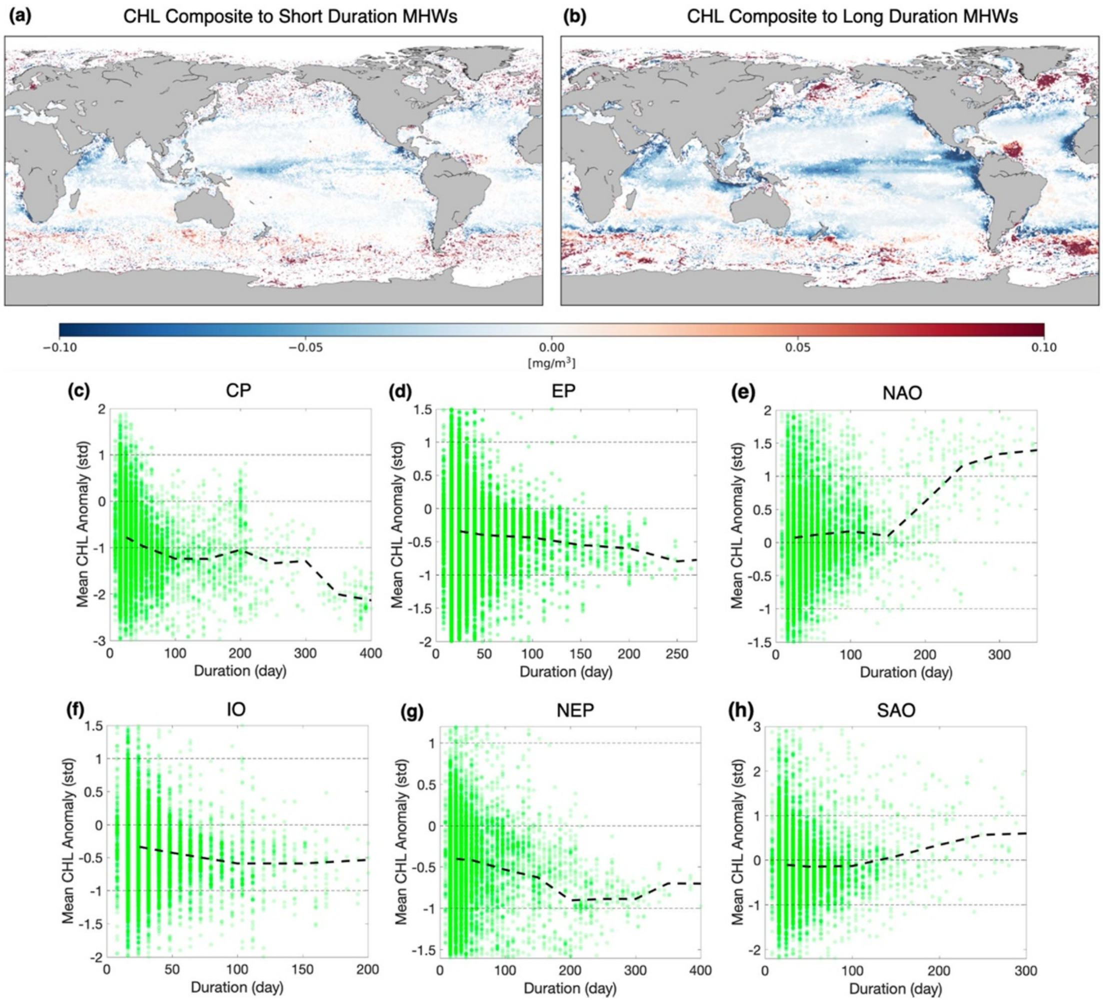

Figure 2. The duration of MHWs controls the intensity of phytoplankton responses. (a), (b) MHW chlorophyll composite on short and long duration. The short and long duration is defined with a mean (μ_{dur}) and standard deviation (σ_{dur}) of duration. Two cases are defined with MHW cases: short duration ($MHW_{dur} < \mu_{dur} - 0.5 \times \sigma_{dur}$) and long duration ($MHW_{dur} > \mu_{dur} + 0.5 \times \sigma_{dur}$). Both chlorophyll composite is used only within significant regions at a 95% confidence level (calculated using a Student's *t*-test). (c)–(h) Scatter plots between maximum chlorophyll anomalies during MHWs, normalized by the standard deviation of chlorophyll and duration at every grid in each selected region where chlorophyll responses to MHWs are significant and strong. The black solid line was calculated by averaging all scatter values with a 50 days moving window.

short persisted MHWs than long persisted MHWs. Based on the relationship between the chlorophyll responses to MHWs and MHWs properties, we suggest that MHW intensity and duration are essential factors in determining the intensity of chlorophyll responses to MHWs.

The most distinctive features of the chlorophyll composite to the MHW (figure 1) are sharp latitudinal changes in both hemispheres, at approximately 50° N and 40° S. The sign of the chlorophyll response to MHWs sharply reverses from a negative at mid-latitudes to positive at high latitudes within these narrow latitudinal bands in both hemispheres. The latitudinal change in the chlorophyll response to MHWs is closely related to the latitudinal contrast of the climatological nitrate concentrations. In the regions where the sign of the MHW-chlorophyll response changes, the climatological mean nitrate gradients are two to six times higher than the global average ranging from 0.007 to 0.02 mmol l^{-1} km^{-1}. The zonal average of the nitrate concentration agrees with that of the composite in chlorophyll anomalies as a response to MHWs in both hemispheres (figures 3(a)–(d)). This result have reassured the importance of background nitrate for MHWs related chlorophyll extremes reported in Hayashida *et al* (2020). The climatological nutrients are critical for chlorophyll responses to MHWs because nitrate is usually insufficient in the tropical and mid-latitude regions due to phytoplankton uptake and poor nutrient supplies from the deep ocean, but abundant in the equatorial eastern Pacific and high-latitude oceans where the micronutrient iron is limited (Moore *et al* 2013, Arteaga *et al* 2014, Bristow *et al* 2017).

To quantify these relationships, we focus on four regions that exhibit rapid meridional transitions in the MHW-chlorophyll response: the North Atlantic Ocean (45°–65° N, 45°–25° W), South Atlantic Ocean (40°–55° S, 0°–60° W), the Agulhas Current region (36°–52° S, 25°–45° E), and Bering Sea

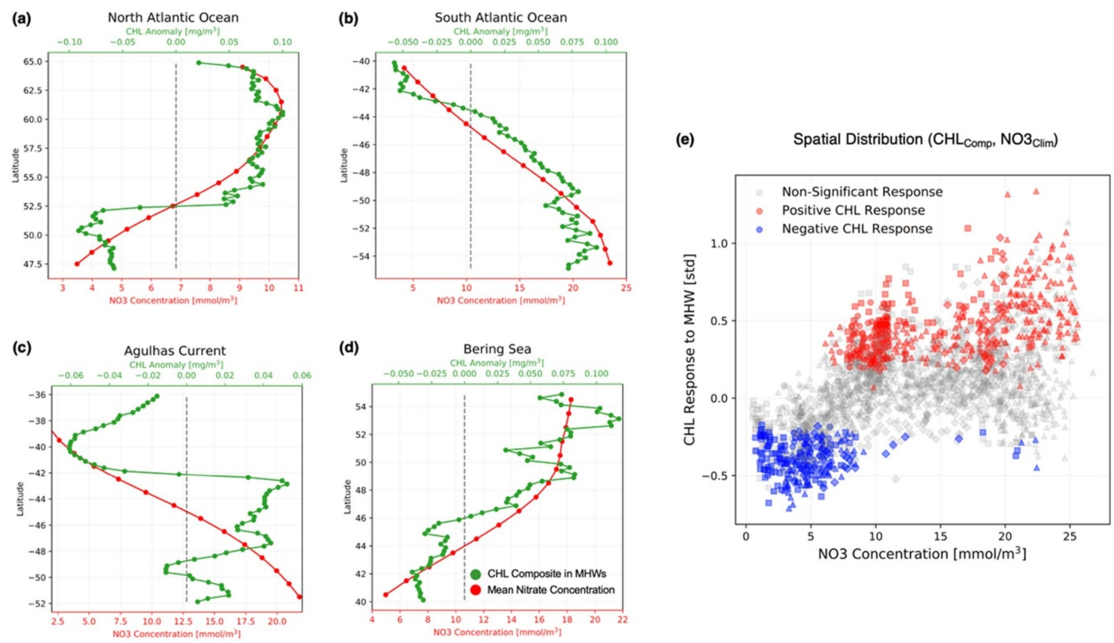

Figure 3. Comparison between nitrate climatology and chlorophyll responses to MHWs. The zonally-averaged climatological mean of nitrate concentration and MHW chlorophyll composites for each region (a)–(d), where the signs of chlorophyll responses to MHWs changed dramatically: (a) NAO (45°–65° N, 25°–55° W); (b) SAO (40°–55° S, 0°–60° W); (c) Agulhas Current (36°–52° S, 25°–45° E); (d) Bering Sea (40°–55° N, 163° E–175° W). (e) Scatter diagram of the normalized chlorophyll composite during MHWs and climatological mean nitrate levels at each grid in four selected regions with different markers: circle (NAO), triangle (SAO), square (Agulhas Current), and diamond (Bering Sea). The blue and red dots represent the negative and positive chlorophyll composites, respectively, whereas the gray dots refer to nonsignificant grid points. Scatter plots of individual regions are provided in the supporting information (figure S7).

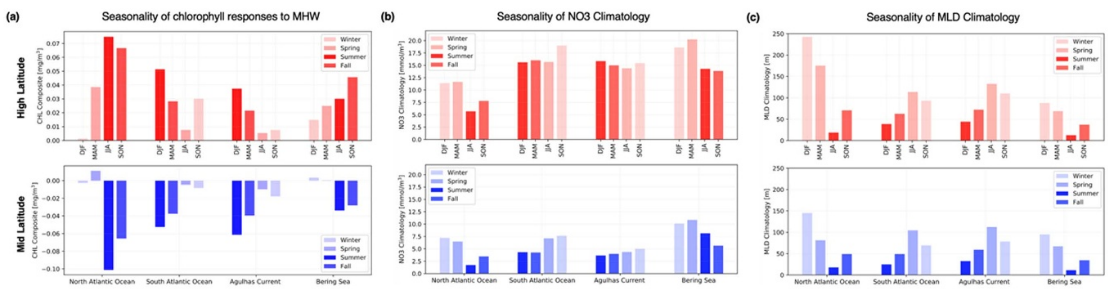

Figure 4. Seasonality of chlorophyll responses to MHWs in the sign of responses changing zone. Seasonality of mean (a) chlorophyll responses to MHW, (b) NO_3 climatology, and (c) MLD climatology averaged on high and mid latitude based on the latitude where the signs of zonally averaged chlorophyll responses were changed. The regions where the latitude ranges from the sign-changing latitude to the end latitude (closer to the north and south pole) for four regions are defined as high latitude and mid latitude vise-versa.

(40°–55° N, 163° E–175° W), and locations of these regions are shown in figure S6. Scatter plots between nitrate concentration climatologies and normalized chlorophyll responses to MHWs at each grid are shown in figure 3(e), where the chlorophyll responses to MHWs changes are distinctive. Positive chlorophyll responses appear in a high nitrate environment, whereas negative chlorophyll responses exist mostly in a low nitrate environment. The sign of the chlorophyll responses to MHWs is changed from negative to positive at approximately 8 mmol m^{-3} nitrate concentration. Based on this scatter analysis, the sign of the MHW chlorophyll composite is well divided by the iso-nitrate lines in figure 1(a). This relationship shows how the abundance of climatological nitrate concentrations determines the different chlorophyll responses to MHWs.

The seasonality of chlorophyll responses to MHWs in the four regions are investigated to further support the importance of interactions between the mixed layer and chlorophyll responses to MHWs. The chlorophyll responses to MHWs show a large seasonal contrast that the stronger positive and negative responses exhibit in the summer and fall than those in the other seasons (figure 4(a)). For the four selected regions, the nitrate concentration in the cold seasons (winter and spring) is relatively less than that in the warm seasons (summer and fall) (figure 4(b)), which is generally supplied by the entrainment from the deep water. The mixed layer is deeper in the cold seasons that the nitrate concentration is relatively abundant compared to nitrate in the warm seasons (figure 4(c)) due to weak thermal convection and wind-driven turbulence, which results in increased light limitations in cold seasons. In the cold seasons, the effects of the MHW-induced stratification, which leads to reduce the nutrient entrainment and enhanced light availability, are weak in the 40°–60° latitudinal band due to strong light limitations. Therefore, the chlorophyll responses to MHWs are weaker in the cold seasons. In contrast, the effects of the mixed-layer shoaling are greater in the warm seasons due to relatively shallower mixed layer that the latitudinal contrast of chlorophyll responses becomes more distinctive (figure 4(a)).

5. Summary and discussion

In this study, we investigate the general pattern of global MHWs related chlorophyll responses using high-resolution satellite-derived global ocean color datasets. MHWs alter contrasting chlorophyll responses to MHWs depending on latitude possibly due to diverse limiting environments. The latitudinal contrast in chlorophyll response to MHWs is observed in a 40°–50° latitudinal zonal bands in both hemispheres except in the northeast Atlantic Ocean where the latitudinal contrast is observed in the 50°–60° latitudinal band. We find that the dramatic changes in the chlorophyll response to MHWs are associated with the location of the strongest meridional gradients in the mean state of nitrate concentrations, suggesting that the background levels of nitrate concentrations are a dominant environmental factor in determining the direction of global chlorophyll response to MHWs. The seasonal contrasts in the chlorophyll responses to MHWs support the impacts of MHW-induced mixed-layer shoaling on phytoplankton.

We have reassured that the chlorophyll responses to MHWs and the relationship between responses and nitrate concentrations, consistent results with recent studies (Gupta Sen *et al* 2020, Hayashida *et al* 2020). Using the model output and satellite observations, previous studies showed chlorophyll anomaly responses for specific regions and in some extreme MHW cases: 23 coastal regions (Hayashida *et al* 2020); 50 extreme MHW events (Gupta Sen *et al* 2020), respectively. Their results for specific regions and global pattern analysis as we shown in the present study lead us to identify the general refinement signal of every MHW case in globally that is closely related to the latitudinal distribution of nitrate concentration and its role in driving chlorophyll extremes. Additionally, showing the spatial similarity between nitrate and chlorophyll responses and the seasonal contrast between warm and cold seasons, we exhibit the distinctive latitudinal contrast of chlorophyll responses and suggest the criteria of nitrate climatology where the sign of chlorophyll responses are changed. Therefore, we can conclude that the relationship between nitrate concentration and MHW-induced chlorophyll response is reinforced by the interaction between the mixed-layer and phytoplankton.

Phytoplankton communities have different growth rates and various nutrients are differently limited to them that responses of plankton functional types (PFTs) to global warming are diverse depending on their compositions (Laufkotter *et al* 2013). It has been reported that the phytoplankton community composition has changed from larger species to smaller pico- and nano-planktons due to strong MHWs in the northeastern Pacific Ocean (Cavole *et al* 2016, Yang *et al* 2018). Specifically, it was predicted that plankton would be much more diverse in the Arctic and Southern Oceans (Ibarbalz *et al* 2019). Further studies are required on phytoplankton responses to MHWs considering the different impacts of each PFT in high-latitude regions.

Global ocean stratification has intensified in recent decades (Li *et al* 2020), projected to reduce surface nitrate concentrations in CMIP5 and CMIP6 simulations (Bopp *et al* 2013, Kwiatkowski *et al* 2020). The background nitrate concentration closely contributes to weak phytoplankton blooming in the tropics and mid-latitudes through interactions between MHW and phytoplankton (Gupta Sen *et al* 2020, Hayashida *et al* 2020). MHWs have been projected to be intensified and occur frequently so that the ecosystem will be more vulnerable to MHWs (Oliver *et al* 2019), implying more severe impacts on marine organisms as MHWs alter other marine ecosystem components, such as coral, seagrass, seabird, and fish colonies, and can further lead to regime shifts in the marine ecosystem (Wernberg *et al* 2012, 2016). Nitrate depletion and intensified MHWs with extended periods may influence the poleward shift of the latitudinal band where the sign of chlorophyll responses to MHW changes or even reverts the positive chlorophyll responses to negative in the high-latitude regions when extreme nitrate depletion occurs in the future climate. Detection and attribution studies in current and future climates are needed to investigate how human activity influences MHW impacts phytoplankton dynamics under the expected more extreme events of future ocean environments (Frölicher *et al* 2018). With potential capabilities of MHWs prediction itself (Jacox *et al* 2022), the prediction of chlorophyll extreme responses to MHWs needs to be developed for providing the early warning forecasts in fisheries and establishing strategies in the global marine ecosystem managements.

Data availability statement

No new data were created or analyzed in this study.

Acknowledgment

The authors thank John P Dunne (NOAA-GFDL) for fruitful discussions in terms of the MHW-related global chlorophyll patterns and anthropogenic chlorophyll responses. The authors appreciate valuable comments for elevating the quality of the manuscript from three anonymous reviewers. This work is supported by the National Research Foundation of Korea (NRF-2021M3I6A1086808) and the project titled '[Korea-Arctic Ocean Observing System (K-AOOS), KOPRI, 20160245]', funded by the MOF, Korea. H-G Lim is supported under Award NA18OAR4320123 from the National Oceanic and Atmospheric Administration, U.S. Department of Commerce. The statements, findings, conclusions, and recommendations are those of the author(s) and do not necessarily reflect the views of the National Oceanic and Atmospheric Administration, or the U.S.

Author contributions

K-M Noh performed the analysis and wrote the manuscript of the paper. J-S Kug, H-G Lim designed the research and wrote the manuscript content. All the authors discussed the results and reviewed the manuscript.

Conflict of interest

The authors declare no competing interests.

Data and code availability

The SST and chlorophyll satellite observation data used in this research are available on www.esrl.noaa.gov/psd/data/gridded/data.noaa.oisst.v2.highres.html and https://esa-oceancolour-cci.org, respectively. The nitrate is provided freely at www.ncei.noaa.gov/access/world-ocean-atlas-2018/. All figures were generated by using software package Python with the matplotlib and basemap modules (https://matplotlib.org/, https://matplotlib.org/basemap/). The map coastlines are derived by the Global Self-consistent, Hierarchical, High-resolution Geography (GSHHG) Database (www.soest.hawaii.edu/pwessel/gshhg/), which has been distributed under the GNU Lesser General Public License and is provided with the basemap Python module.

ORCID iDs

Kyung Min Noh https://orcid.org/0000-0003-4233-4490
Hyung-Gyu Lim https://orcid.org/0000-0002-0746-5332
Jong-Seong Kug https://orcid.org/0000-0003-2251-2579

References

Amaya D J, Miller A J, Xie S-P and Kosaka Y 2020 Physical drivers of the summer 2019 North Pacific marine heatwave *Nat. Commun.* **11** 1903
Arias-Ortiz A *et al* 2017 A marine heat wave drives massive losses from the world's largest seagrass carbon stocks *Nat. Clim. Change* **8** 338–44
Arteaga L, Pahlow M and Oschlies A 2014 Global patterns of phytoplankton nutrient and light colimitation inferred from an optimality-based model *Glob. Biogeochem. Cycles* **28** 648–61
Banzon V, Smith T M, Chin T M, Liu C and Hankins W 2016 A long-term record of blended satellite and *in situ* sea-surface temperature for climate monitoring, modeling and environmental studies *Earth Syst. Sci. Data* **8** 165–76
Behrenfeld M J, Boss E S, Siegel D A and Shea D M 2005 Carbon-based ocean productivity and phytoplankton physiology from space *Glob. Biogeochem. Cycles* **19** 57–14
Blondeau-Patissier D, Gower J F R, Dekker A G, Phinn S R and Brando V E 2014 A review of ocean color remote sensing methods and statistical techniques for the detection, mapping and analysis of phytoplankton blooms in coastal and open oceans *Prog. Oceanogr.* **123** 123–44
Bond N A, Cronin M F, Freeland H and Mantua N 2015 Causes and impacts of the 2014 warm anomaly in the NE Pacific *Geophys. Res. Lett.* **42** 3414–20
Bopp L *et al* 2013 Multiple stressors of ocean ecosystems in the 21st century: projections with CMIP5 models *Biogeosciences* **10** 6225–45
Bristow L A, Mohr W, Ahmerkamp S and Kuypers M M M 2017 Nutrients that limit growth in the ocean *Curr. Biol.* **27** R474–8
Cavole L *et al* 2016 Biological impacts of the 2013–2015 warm-water anomaly in the Northeast Pacific: winners, losers, and the future *Oceanography* **29** 1–14
Cheung W W L and Frölicher T L 2020 Marine heatwaves exacerbate climate change impacts for fisheries in the northeast Pacific *Sci. Rep.* **10** 6678
di Lorenzo E and Mantua N 2016 Multi-year persistence of the 2014/15 North Pacific marine heatwave *Nat. Clim. Change* **6** 1042–7
Doney S C 2006 Plankton in a warmer world *Nature* **444** 695–6
Frölicher T L, Fischer E M and Gruber N 2018 Marine heatwaves under global warming *Nature* **560** 1–17
Garcia H E *et al* 2018 *World Ocean Atlas 2018, Volume 4: Dissolved Inorganic Nutrients (Phosphate, Nitrate and Nitrate+Nitrite, Silicate)* ed A Mishonov, NOAA Atlas NESDIS 84 p 35
Garrabou J *et al* 2009 Mass mortality in Northwestern Mediterranean rocky benthic communities: effects of the 2003 heat wave *Glob. Change Biol.* **15** 1090–103
Gruber N, Boyd P W, Frölicher T L and Vogt M 2021 Biogeochemical extremes and compound events in the ocean *Nature* **600** 395–407
Gupta Sen A *et al* 2020 Drivers and impacts of the most extreme marine heatwaves events *Sci. Rep.* **10** 19359
Hayashida H, Matear R J and Strutton P G 2020 Background nutrient concentration determines phytoplankton bloom response to marine heatwaves *Glob. Change Biol.* **26** 4800–11
Hobday A J *et al* 2016 A hierarchical approach to defining marine heatwaves *Prog. Oceanogr.* **141** 227–38
Hobday A J *et al* 2018 Categorizing and naming marine heatwaves *Oceanography* **31** 162–73
Holbrook N J *et al* 2019 A global assessment of marine heatwaves and their drivers *Nat. Commun.* **10** 2624

Hughes T P *et al* 2017 Global warming and recurrent mass bleaching of corals *Nature* **543** 373–7

Ibarbalz F M *et al* 2019 Global trends in marine plankton diversity across kingdoms of life *Cell* **179** 1084–97.e21

Jacox M G, Alexander M A, Amaya D, Becker E, Bograd S J, Brodie S, Hazen E L, Buil M P and Tommasi D 2022 Global seasonal forecasts of marine heatwaves *Nature* **604** 486–502

Jones T *et al* 2018 Massive mortality of a planktivorous seabird in response to a marine heatwave *Geophys. Res. Lett.* **45** 3193–202

Kwiatkowski L *et al* 2020 Twenty-first century ocean warming, acidification, deoxygenation, and upper-ocean nutrient and primary production decline from CMIP6 model projections *Biogeosciences* **17** 3439–70

Laufkotter C, Vogt M and Gruber N 2013 Long-term trends in ocean plankton production and particle export between 1960–2006 *Biogeosciences* **10** 7373–93

le Grix N, Zscheischler J, Laufkötter C, Rousseaux C S and Frölicher T L 2021 Compound high-temperature and low-chlorophyll extremes in the ocean over the satellite period *Biogeosciences* **18** 2119–37

Lee S, Park M-S, Kwon M, Kim Y H and Park Y-G 2020 Two major modes of East Asian marine heatwaves *Environ. Res. Lett.* **15** 074008

Li G, Cheng L, Zhu J, Trenberth K E, Mann M E and Abraham J P 2020 Increasing ocean stratification over the past half-century *Nat. Clim. Change* **10** 1116–23

Li Y, Ren G, Wang Q and You Q 2019 More extreme marine heatwaves in the China Seas during the global warming hiatus *Environ. Res. Lett.* **14** 104010

McCabe R M, Hickey B M, Kudela R M, Lefebvre K A, Adams N G, Bill B D, Gulland F M D, Thomson R E, Cochlan W P and Trainer V L 2016 An unprecedented coastwide toxic algal bloom linked to anomalous ocean conditions *Geophys. Res. Lett.* **43** 10336–76

Moore C M *et al* 2013 Processes and patterns of oceanic nutrient limitation *Nat. Geosci.* **6** 1–10

Oliver E C J *et al* 2018 Longer and more frequent marine heatwaves over the past century *Nat. Commun.* **9** 1324

Oliver E C J *et al* 2019 Projected marine heatwaves in the 21st century and the potential for ecological impact *Front. Mar. Sci.* **6** 1–12

Oliver E C J, Benthuysen J A, Bindoff N L, Hobday A J, Holbrook N J, Mundy C N and Perkins-Kirkpatrick S E 2017 The unprecedented 2015/16 Tasman Sea marine heatwave *Nat. Commun.* **8** 16101

Pearce A, Lenanton R, Jackson G, Moore J, Feng M and Gaughan D 2011 The 'marine heat wave' off Western Australia during the summer of 2010/11 *Fisheries Research Report* No. 222 (Western Australia: Department of Fisheries) p 40

Reynolds R W, Smith T M, Liu C, Chelton D B, Casey K S and Schlax M G 2007 Daily high-resolution-blended analyses for sea surface temperature *J. Clim.* **20** 5473–96

Roberts S D, van Ruth P D, Wilkinson C, Bastianello S S and Bansemer M S 2019 Marine heatwave, harmful algae blooms and an extensive fish kill event during 2013 in South Australia *Front. Mar. Sci.* **6** 1–20

Rodrigues R R, Taschetto A X A S, Gupta A and Foltz G R 2019 Common cause for severe droughts in South America and marine heatwaves in the South Atlantic *Nat. Geosci.* **12** 1–9

Sarmiento J L *et al* 2004 Response of ocean ecosystems to climate warming *Glob. Biogeochem. Cycles* **18** GB3003

Smale D A *et al* 2019 Marine heatwaves threaten global biodiversity and the provision of ecosystem services *Nat. Clim. Change* **9** 1–10

Valente A *et al* 2016 A compilation of global bio-optical *in situ* data for ocean-colour satellite applications *Earth Syst. Sci. Data* **8** 235–52

Vogt L, Burger F A, Griffies S M and Frölicher T L 2022 Local drivers of marine heatwaves: a global analysis with an earth system model *Front. Mar. Sci.* **4** 847995

Wernberg T *et al* 2016 Climate-driven regime shift of a temperate marine ecosystem *Science* **353** 169–72

Wernberg T, Smale D A, Tuya F, Thomsen M S, Langlois T J, de Bettignies T, Bennett S and Rousseaux C S 2012 An extreme climatic event alters marine ecosystem structure in a global biodiversity hotspot *Nat. Clim. Change* **5** 1–5

Woolway R I, Kraemer B M, Zscheischler J and Albergel C 2021 Compound hot temperature and high chlorophyll extreme events in global lakes *Environ. Res. Lett.* **16** 124066

Yang B, Emerson S R and Peña M A 2018 The effect of the 2013–2016 high temperature anomaly in the subarctic Northeast Pacific (the 'Blob') on net community production *Biogeosciences* **15** 6747–59